coatings

Supplementary Materials: Simple and Rapid Preparation of MIL-121 with Small Particles for Lithium Adsorption from Brine

Qinyan Wei, Bingqian Shi, Fei Wang, Shuoshuo Shao, Liang Zhu * and Xiaoyu Zhao *

College of Chemical Engineering and Materials Science, Tianjin University of Science & Technology, Tianjin 300457, China; weiqy@mail.tust.edu.cn (Q.W.); shibq@mail.tust.edu.cn (B.S.); yifei@mail.tust.edu.cn (F.W.); woshihuaidan83@mail.tust.edu.cn (S.S.)
* Correspondence: zhuliang@tust.edu.cn (L.Z.); xyz@tust.edu.cn (X.Z.)

Note S1. SEM Characterizations of the product under different sodium hydroxide addition conditions

Figure S1 The quality of the product obtained by adding 2 mmol of NaOH solution was 0.240 g and the morphology was extremely uneven. The quality of the product obtained by adding 4 mmol of NaOH solution was 0.598 g. Scanning electron microscope showed that the maximum particle size of the sample was less than 5 μm, and the morphology was polyhedral. The mass of the product obtained by adding 8 mmol of NaOH solution is 0.617 g, and the maximum particle size of the sample is less than 5 μm. After adding 16 mmol of NaOH solution to the reaction, it becomes gelatinous as shown in Figure **S1b**. The centrifugal speed of 12000 still could not be separated, and the powder product was obtained by direct drying for 72 hours. The quality of the product is 2.72 g, the sample size is greater than 50 μm, and it is a long strip.

Note S2. FTIR, Raman Characterizations of the product under different sodium hydroxide addition conditions

Figure S2 When the sodium hydroxide addition amount is less than 8 mmol, the Raman spectrum peak of the product is consistent with the MIL-121 Raman spectrum peak. When the addition amount is greater than 8 mmol, the characteristic peaks of MIL-121 at 798 cm^{-1}, 812 cm^{-1}, and 825 cm^{-1} disappear. Combined with SEM characterization and yield, it can be determined that the optimal addition amount of sodium hydroxide is 4 mmol.

Note S3. Raman spectrum analysis of standards

Figure S3 Raman analysis was performed on $Al(NO_3)_3 \cdot 9H_2O$, H_4BTEC, carboxylic acid hydrate and MIL-121. Using the same test conditions, the spectral information was collected at a Raman shift of 250~4000 cm^{-1}, and then the origin software was used to perform baseline subtraction and peak finding processing as shown in **Figure S3**.

From the analysis of the Raman spectra of **Figure S3b** pyromellitic acid and comparing the carboxylic acid compounds with the existing Raman standard spectra, it can be concluded that the benzene ring in pyromellitic acid is pulled by four carboxyl groups. The moderately strong peak at 1332 cm^{-1} is the C-C stretching vibration peak. The medium intensity peak at 3092 cm^{-1} is the C-H stretching vibration peak on the benzene ring. The weak peak at 1127 cm^{-1} is the characteristic peak of bending vibration in the plane H. The weak peak at 799 cm^{-1} is the vibration peak of the hydroxyl group on the carboxylic acid. The medium-strength peaks at 1283 cm^{-1}, 1341 cm^{-1}, and 276 cm^{-1} are C-O stretching vibration peaks. 1305 cm^{-1} is the stretching vibration peak of C-H. 1782 cm^{-1} and 1870 cm^{-1} are C=O stretching vibration peaks. 708 cm^{-1} and 756 cm^{-1} are the characteristic peaks of flexural vibration from the plane H outward. 495 cm^{-1} and 646 cm^{-1} are the flexural vibration peaks of C-H.

Figure S3c is the Raman spectrum analysis of the carboxylic acid hydrate. It can be seen that the characteristic peak of the benzene ring becomes weaker and the peak position shifts to the high Raman shift after the carboxylic acid is coordinated with water. Compared with pyromellitic acid, the characteristic peak of bending vibration in the plane H

Citation: Wei, Q.; Shi, B.; Wang, F.; Shao, S.; Zhu, L.; Zhao, X. Simple and Rapid Preparation of MIL-121 with Small Particles for Lithium Adsorption from Brine. *Coatings* **2021**, *11*, 854. https://doi.org/10.3390/coatings11070854

Academic Editor: Mazeyar Parvinzadeh Gashti

Received: 29 May 2021
Accepted: 8 July 2021
Published: 16 July 2021

has shifted from 1127 cm^{-1} to 1172 cm^{-1}. The vibration peak of the hydroxyl group on the carboxylic acid shifted from 799 cm^{-1} to 817 cm^{-1}. The characteristic peak of flexural vibration outside the plane H of 756 cm^{-1} is translated to 771 cm^{-1}.

Figure S3d shows the Raman spectrum analysis of the prepared MIL-121. By comparing with the Raman characteristic peaks of the raw materials used in the synthesis of aluminum nitrate nonahydrate, pyromellitic acid and water, it can be seen that MIL-121 has new strong characteristic peaks at 295 and 316 cm^{-1}. This is due to Al-O stretching vibration. Compared with pyromellitic acid, the characteristic peaks of the benzene ring and carboxyl group in MIL-121 shifted to a higher wave number. For example, the medium-strength peak of 1463 cm^{-1} is the C-C stretching vibration peak, which has moved 131 cm^{-1} compared to the C-C stretching vibration peak of the ligand 1332 cm^{-1}.

Note S2. The adsorption performance test data of MIL-121 after polymerization obtained under different experimental conditions

Table S 5 The adsorption capacity is calculated using the following formula [1]:

$$\text{capacity}(\text{mmol} \cdot g^{-1}) = \frac{C \times V}{M_w \times w}$$

C is the difference in solution concentration before and after adsorption, V is the volume of lithium chloride salt solution, is the molar mass of lithium chloride, w is the mass of the polymerized sample.

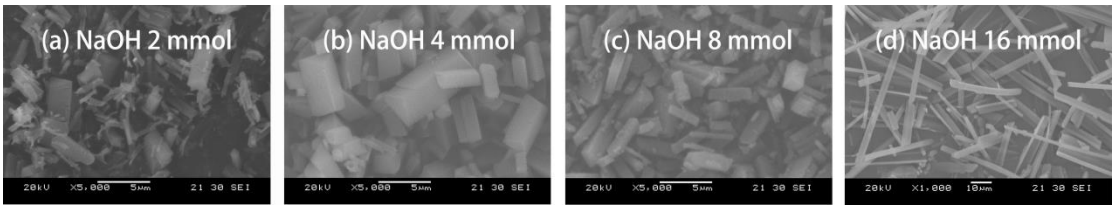

Figure S1. SEM images of products under different sodium hydroxide addition conditions.

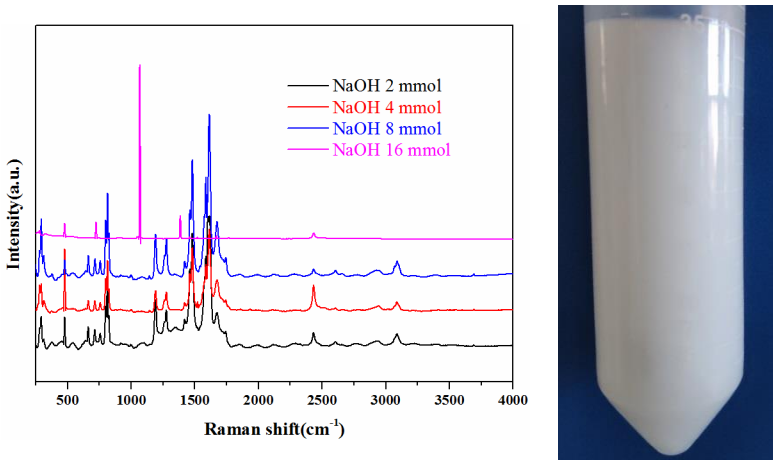

(**a**) (**b**)

Figure S2. (**a**) Raman diagram of products with different sodium hydroxide addition levels, (**b**) Centrifugation results of products with addition volume of 16 mmol.

Table S1. Peaks location of PXRD pattern and the crystal indices of MIL-121 [2], MIL-121-80 °C NaOH 4mmol.

No	Peak Position		Interplaner spacing	FWHM	Miller indices
	Ref.MIL-121	2 Theta(°)	d(Å)	—	(hkl)
1	8.506	8.463	10.440	0.19341	-110
2	10.964	10.905	8.106	0.19314	200
3	13.030	12.965	6.823	0.22761	020
4	14.797	14.735	6.007	0.19466	-1-11

5	17.060	17.012	5.208	0.19191	-220
6	19.503	19.413	4.569	0.25942	0-21
7	22.030	21.961	4.044	0.25366	400
8	25.117	24.986	3.561	0.39297	2-21
9	25.710	25.635	3.472	0.28133	-330
10	26.309	26.164	3.403	0.28742	1-31
11	29.849	29.781	2.998	0.25446	-2-22
12	32.756	32.541	2.749	0.33619	3-31

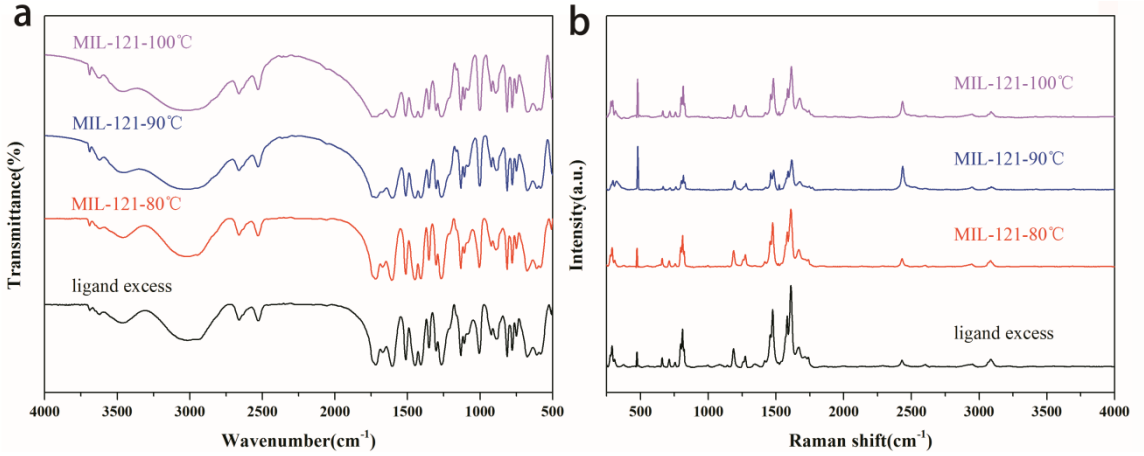

Figure S3. (**a**) FTIR spectrum of MIL-121 and (**b**) Raman spectrum of MIL-121.

Table S2. The particle size distribution of MIL-121 under different temperature.

	MIL-121-80 °C	**MIL-121-90 °C**	**MIL-121-100 °C**
mean(μm)	2.55	3.80	4.11
median(μm)	2.15	3.37	3.94
C.V.	61.29	62.52	64.91
D10(μm)	0.85	1.03	0.97
d50(μm)	2.15	3.37	3.94
d90(μm)	4.92	7.31	7.39

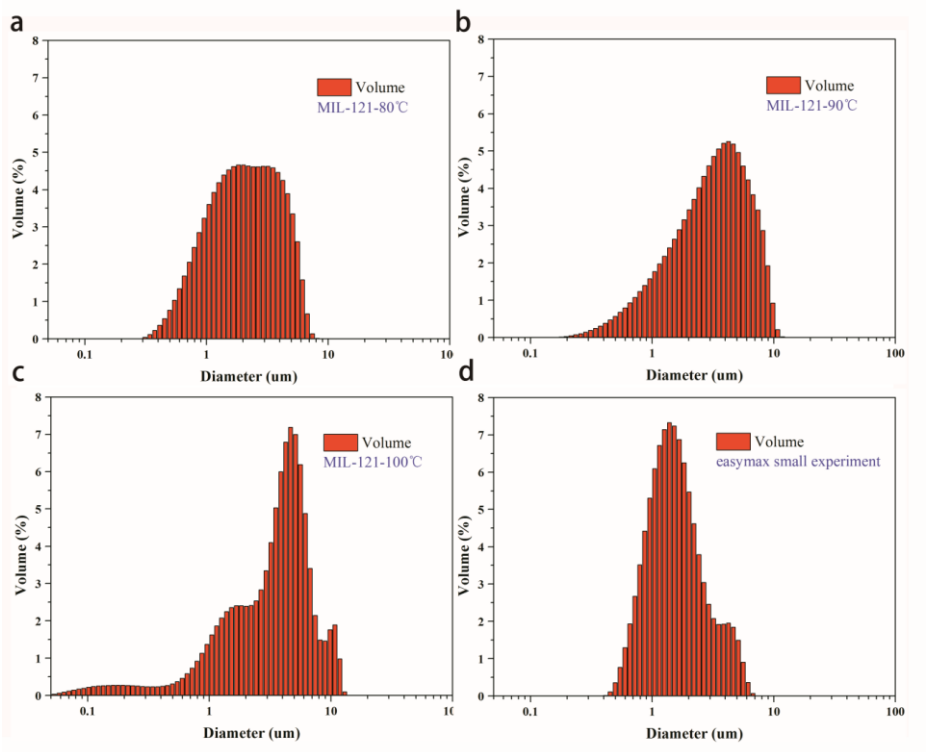

Figure S4. Size distribuation of (**a**) MIL-121-80 °C, (**b**) MIL-121-90 °C, (**c**) MIL-121-100 °C, (**d**) MIL-121-easymax small experiment.

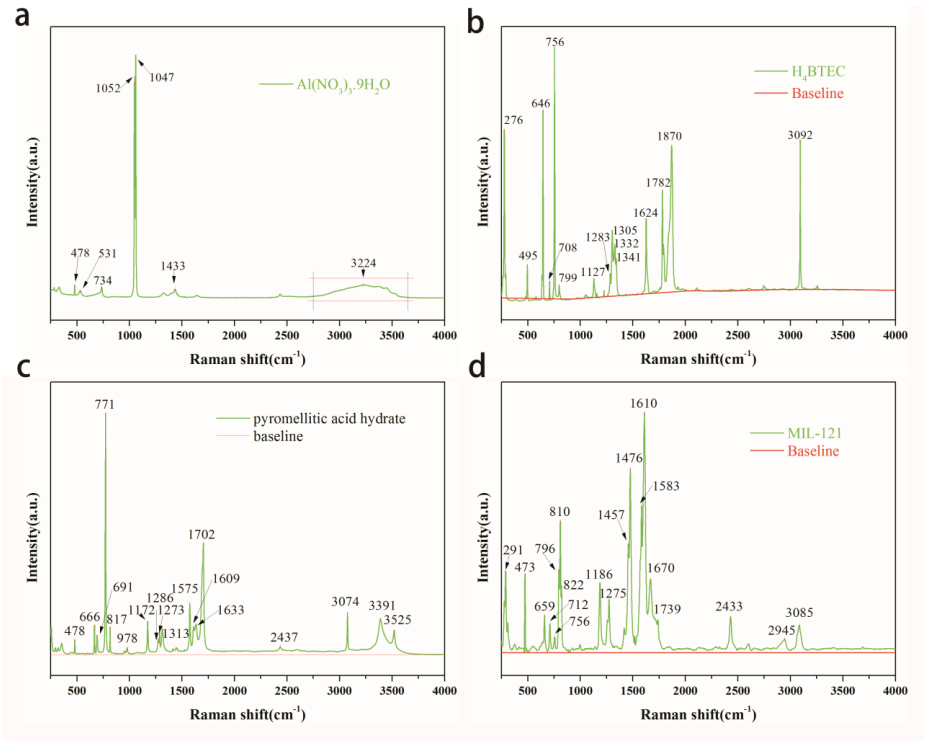

Figure S5. Raman spectras of (**a**)Al(NO3)3 9H2O,(**b**) H4BTEC,(**c**) pyromellitic acid hydrate,(**d**) MIL-121.

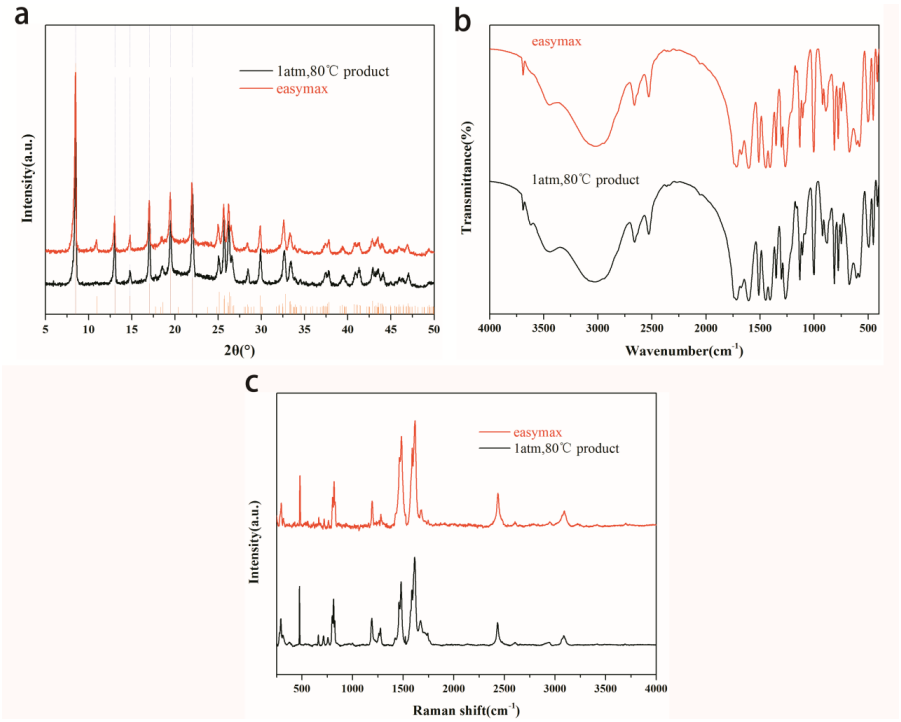

Figure S6. (**a**) PXRD pattern of MIL-121-(1atm,80 °C), easymax product, (**b**) FTIR spectrum of MIL-121-(1atm,80 °C), easymax product and (**c**) Raman spectrum of MIL-121-(1atm,80 °C), easymax product.

Table S3. Preparation method and preparation time of partial aluminum-based MOF.

material	Preparation time	Preparation method	T/K	references
MOF-303	24	hydrothermal	100	[3]
PCN-332	12	solvothermal	423.15	[4]
PCN-333	24	solvothermal	408.15	[4]
MOF-253	24	solvothermal	393.15	[5]
MIL-101-NH_2	72	solvothermal	403.15	[6]
MIL-53	5h	hydrothermal	423	[7]
MIL-96(Al)	2	hydrothermal	483.15	[8]
MIL-121	21	hydrothermal	483.15	[2]
MIL-68	18	solvothermal	403	[9]
MIL-100	72	hydrothermal	483	[10]
NH_2-MIL-53	5	hydrothermal	423.15	[11]

Table S4. TGA mass loss of N-MIL-121 crystals synthesized under different conditions.

Temperature ℃	Weight(%)				
	Hydrothermal 80℃	Hydrothermal 90℃	Hydrothermal 100℃	1atm,80℃	easymax
25	0.21	0.06	1.77	0.06	0
50	1.24	1.10	2.2	0.68	0.29
80	4.38	2.68	3.13	3.24	1.32
100	5.22	3.19	3.7	4.83	1.89
200	6.32	3.65	4.51	6.05	2.54
250	8.33	5.28	6.03	7.62	4.33

280	9.06	5.98	6.73	8.08	5.20
300	9.36	6.32	6.94	8.42	5.52
320	9.74	6.85	7.19	8.80	5.85
350	10.89	9.06	8.07	9.90	6.72
380	13.2	14.85	10.62	13.07	9.18
400	16.01	20.21	13.80	17.71	12.51
420	20.60	25.99	18.18	24.87	17.21
450	29.5	32.76	26.23	34.64	26.63
480	35.27	38.98	31.8	40.93	32.75
500	39.96	44.03	38.1	46.12	38.61
520	45.70	48.38	45.21	49.56	45.73
550	52.25	52.05	49.74	54.05	50.33
580	58.07	56.5	54.58	59.58	55.89
600	62.61	59.89	57.94	63.85	59.95
620	66.15	62.43	60.29	67.14	62.77
650	68.77	64.35	62.07	69.51	64.87
680	69.99	64.99	62.70	70.65	65.57
720	71.08	65.29	63.09	71.70	66.02
780	72.27	65.49	65.50	72.90	66.53

Table S5. The adsorption performance test data of MIL-121 after polymerization obtained under different experimental conditions.

sample	Salt solution	Standard solution ion concentration （mg/L）	Ion concentration after adsorption (mg/L)	Concentration difference /(mg▪L^{-1})	Adsorption capacity /(mmol▪g^{-1})
MIL-121-80 °C	LiCl	15.296	14.755	0.541	0.185
MIL-121-90 °C	LiCl	15.296	14.746	0.550	0.188
MIL-121-100 °C	LiCl	15.296	14.736	0.560	0.192
100 mL	LiCl	15.296	14.764	0.532	0.182
250 mL	LiCl	15.296	14.774	0.522	0.179

References

1. Ou, R.; H. Zhang, J.; Wei, S.; Kim, L.; Wan, N.S.; Nguyen, Y.; Hu, X.; Zhang, G.; Simon, P.; Wang, H. Thermoresponsive amphoteric metal-organic frameworks for efficient and reversible adsorption of multiple salts from water. *Adv. Mater.* 2018, *30*, 1802767.
2. Volkringer, C.; Loiseau, T.; Guillou, N.; Ferey, G.; Haouas, M.; Taulelle, F.; Elkaim, E.; Stock, N. High-throughput aided synthesis of the porous metal-organic framework-type aluminum pyromellitate, Mil-121, with extra carboxylic acid functionalization. *Inorg. Chem.* 2010, *49*, 9852−62.
3. Fathieh, F.; Kalmutzki, M.J.; Kapustin, E.A.; Waller, P.J.; Yang, J.; Yaghi, O.M. Practical water production from desert air. *Sci. Adv.* 2018, *4*; https://advances.sciencemag.org/content/4/6/eaat3198.short
4. Feng, D.; Liu, T.F.; Su, J.; Bosch, M.; Wei, Z.; Wan, W.; Yuan, D.; Chen, Y.P.; Wang, X.; Zhou, H.C. Stable metal-organic frameworks containing single-molecule traps for enzyme encapsulation. *Nat Commun* 2015, *6*, 1−8
5. Duan, H.; Zeng, Y.; Yao, X.; Xing, P.; Liu, J.; Zhao, Y. Tuning synergistic effect of Au–Pd bimetallic nanocatalyst for aerobic oxidative carbonylation of amines. *Chemistry of Materials* 2017, *29*, 3671−77.
6. Lin, C.; Zou, Z.; Lei, Z.; Wang, L.; Song, Y. Fluorescent metal-organic frameworks Mil-101(Al)-Nh2 for rapid and sensitive detection of ellagic acid. *Spectrochim. Acta, Part A Mol. Biomol. Spectrosc.* 2020, *242*, 118739.
7. Wang, M.; Zhang, X.; Chen, Y.; Zhang, A. Estimation of the desorption energy of dichloromethane and water in Mil-53 by Dsc and Ab-initio calculations. *Sci. Chin. Chem.* 2016,*59*, 398−404.
8. Knebel, A.; Friebe, S.; Bigall, N.C.; Benzaqui, M.; Serre, C.; Caro, J. Comparative study of Mil-96(Al) as continuous metal-organic frameworks layer and mixed-matrix membrane." *ACS Appl. Mater. Interfaces* 2016, *8*, 7536−44.
9. Wu, S.C.; You, X.; Yang, C.; Cheng, J.H. Adsorption behavior of methyl orange onto an aluminum-based metal organic framework, Mil-68(Al). *Water Sci Technol* 2017, *75*, 2800−10.
10. Khan, A.H.; Barth, B.; Hartmann, M.; Haase, J.; Bertmer, M. Nitric oxide adsorption in Mil-100(Al) Mof studied by solid-state Nmr. *J. Phys. Chem. C* 2018, *122*, 12723−30.
11. Lu, T.; Song, H.; Dong, X.; Hu, J.; Lv, Y. "A highly selective and fast-response photoluminescence humidity sensor based on F− decorated Nh2-Mil-53(Al) nanorods. *J. Mater. Chem. C* 2017, *5*, 9465−71.